



ELSEVIER

Contents lists available at SciVerse ScienceDirect

Journal of Alloys and Compounds

journal homepage: www.elsevier.com/locate/jallcom

Formation of Al–Fe–Si glass that grows from the melt through a first-order transition

L.A. Bendersky^{a,*}, F. Mompiou^b^a Material Measurement Laboratory, National Institute of Standards and Technology, Gaithersburg, MD 20899, USA^b Centre d'Élaboration de Matériaux et d'Études Structurales, CNRS, Toulouse 31055, France

ARTICLE INFO

Article history:

Received 22 June 2011

Received in revised form 9 January 2012

Accepted 10 January 2012

Available online xxx

Keywords:

Metallic glass

Al–Fe–Si

TEM

Rapid solidification

ABSTRACT

Microstructures of rapidly solidified Al–Fe–Si alloys demonstrate possible formation of a glassy phase, which we term q-glass, that is not a kinetically frozen liquid. Microstructural observations point out that the phase grows from the melt by a first order phase transition in the manner of a crystal, but scatters as a metallic glass. In this paper, by studying a large number of Al–Fe–Si alloys (8–22 at% Fe and 5–20 at% Si), we confirmed this observation and identified domains of formation of the q-glass as a primary phase, as well as a 1/1 α -cubic approximant and an icosahedral phase. Our attempts to grow such a glass in different metallic systems by substituting Fe with Ni and Co have not succeeded. We discuss several reasons why the Al–Fe–Si system might be unique.

© 2012 Published by Elsevier B.V.

1. Introduction

A metallic glass that forms from a melt by an apparent first-order transformation has been reported for Al-rich Al–Fe–Si rapidly solidified (RS) alloys [1–3]. Claims of the nature of the transformation were based on transmission electron microscopy (TEM) micrographs of the solidified microstructure showing nodules of glassy phase surrounded by a duplex structure of the glass and aluminum. The morphology is of a typical hypereutectic structure where the first phase to form from a melt, the glass, comes as the nodules; and then depletion of the melt in Fe results in the formation of a duplex Al + glass structure. Composition of the glass nodules in the e-beam surface melted Al–7Fe–2Si at% alloy was measured by energy dispersive spectroscopy (EDS) as Al–22Fe–2Si at% and Al–4Fe–2Si at% on average for the duplex matrix [4]. Because this isotropic glass has been obtained from the melt by a growth process allowing atomic rearrangements at the interface, and not from a kinetically frozen liquid, the glass was coined q-glass (QG) [3]. One hundred percent glass in the composition Al₇₀Fe₁₃Si₁₇ has been observed by Suzuki et al. [5] and Legresy et al. [6] in melt spun ribbons.

In this paper we look for answers to the following questions: (1) is the reported 100% Al–Fe–Si glass a kinetically frozen melt or a structure that was formed by the coalescence of growing QG nodules (boundaries of which would be indistinguishable in TEM) and (2) how substituting Fe with different transition metals (TM) could

affect the formation of QG by nucleation and growth. To address these questions we examined by TEM and XRD a large number of rapidly solidified Al–Fe–Si alloys with compositions ranging from 8 to 22 at% Fe and 5 to 20 at% Si. For the AlFeSi compositions that exhibit formation of QG, Fe was substituted by Ni and Co either completely or partially and the alloys were prepared by the same RS techniques and conditions.

2. Experimental

Al–Fe–Si alloys with compositions 5/8, 10/13, 13/17, 15/20, 20/20, 18/22, 13/23, 15/10 and 18/8 (i.e. 5/8 stands for Al–5Fe–8Si at%) were prepared by arc melting pure 99.99% Al, 99.99% Fe and 99.99% Si and melt spinning on a Cu wheel (diameter 40 cm, wheel speed 3000 rpm) under He atmosphere. Al–Ni–Si and Al–Co–Si alloys with similar compositions (Fe exchanged for Ni or Co) were prepared similarly. The very brittle flakes/ribbons were prepared for TEM by ion-milling using a LN₂ cold stage.

3. Results

General remark: Observation of many ribbons microstructures show a poor reproducibility, which is strongly affected by variability of cooling conditions and the narrow temperature windows for different metastable reactions. Because of a large number of equilibrium and metastable phases in the Al-rich corner of the Al–Fe–Si system the formation of several phases are in competition in the undercooled melts; thus the observed microstructural variations.

For the four compositions 5/8, 10/13, 13/17 and 15/20, the QG coexists with (Al) (Fig. 1a). For the highest Al (5/8 alloy) concentration the QG appears as an intercellular secondary phase; for the

* Corresponding author.

E-mail address: leoben@nist.gov (L.A. Bendersky).

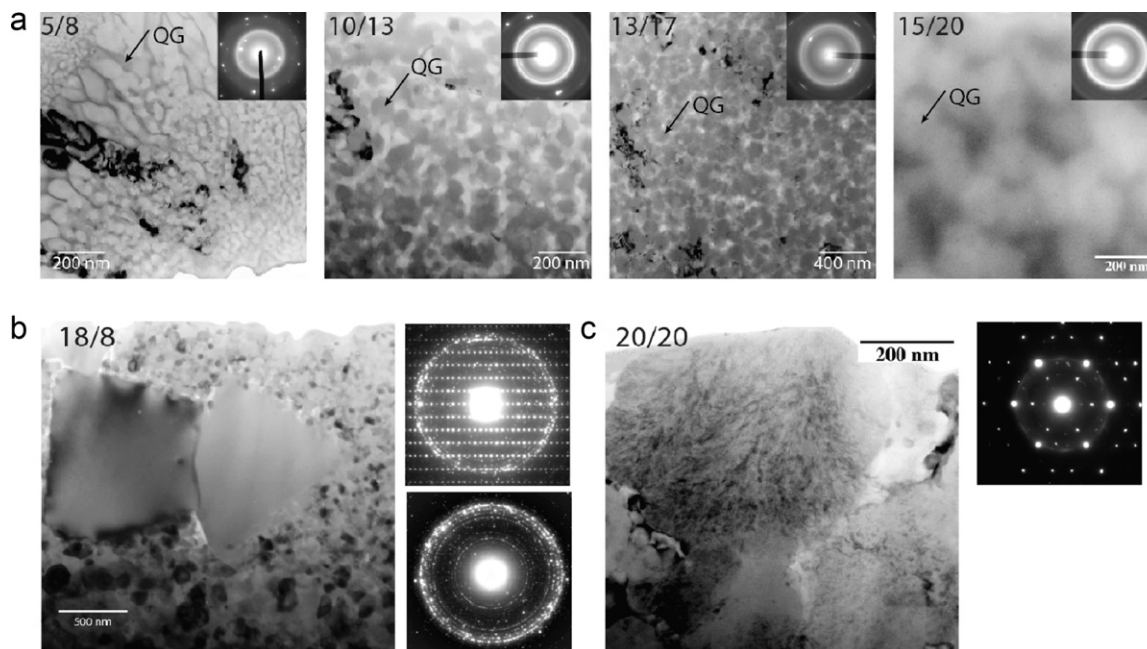


Fig. 1. Bright field TEM micrographs of different AlFeSi alloys: (a) 5/8, 10/13, 13/17 and 15/20 showing formation of QG; (b) 18/8 showing formation of stable β -phase and metastable α -phase; (c) 20/20 showing nodules of defected icosahedral phase.

compositions with lower Al the QG forms as isolated nodules separated by a layer of (Al), supporting formation of the glassy phase as the first phase to solidify. The volume fraction of QG gradually increases with the increase in Fe and Si; and for Fe concentrations higher than 13 at% the QG coalesces and forms a 100% glassy structure. These microstructural observations are typical of hypo and hypereutectic alloys where the (Al) and QG are the end phases. Even if the glassy phase appears as a single phase for the 15/20 alloy, there is microstructural evidence that the phase was also formed by nucleation and growth: contrast variations observed for this alloy are due to compositional variation resulting from a coring at the periphery of impinging nodules. Occasionally, the 100% glass was also observed in the 13/17 alloys that was reported earlier [5,6].

Fig. 2 shows SEM images of ribbons' cross-sections for different samples of the 15/20 alloys. The structure in Fig. 2a consists of large elongated grains of a crystalline phase; this is not a typical structure. Fig. 2b shows a uniform contrast across the ribbon that suggests a 100% glass structure. Fig. 2c shows variation in the contrast, uniform on the wheel side (highest cooling rate, a melt in contact with a cooling Cu wheel) and non-uniform at the upper part. In this sample apparently the complete coalescence of the QG occurred at the bottom part, and partial with segregated Al – at the slower cooled upper part. The SEM results were supported by TEM observation.

Structural variations could be also found within the sample that appears as 100% glass by XRD or SEM. An example of such variations

is shown in Fig. 3, where dark field images (placing selected area aperture over the diffraction ring of strongest intensity, Fig. 3b) and corresponding diffraction patterns (SAED) were taken from three thin areas A (Fig. 3e), B (Fig. 3d) and C (Fig. 3c) around the perforated hole in the TEM specimen. The dark field image from the area A shows a smooth contrast, typical for a metallic glass, with very fine speckling. The speckling size increases progressively moving from A to C area and the continuous diffuse diffraction rings of a glassy structure become spotty in C consistent with a polycrystalline structure. Microdiffraction patterns taken from isolated grains in area C show that the grains belong to the b.c.c. α -phase ($Im\bar{3}$, $a = 1.256$ nm [7]), which is metastable in Al–Fe–Si [8–10], and stable with a slightly different structural modification ($Pm\bar{3}$, $a = 1.264$ nm) in Al–Mn–Si [11]. This phase can be seen as a 1/1 cubic approximant of an icosahedral quasicrystal with near-icosahedral Mackey clusters assembled in bcc lattice nodes [11]. Such evolution of glass into nanocrystals of the α -phase was also observed in $Al_{70}Fe_{13}Si_{17}$ surface-melted alloys for lower velocities (lower cooling rates) of electron beam scanning [12].

Based on these observations, we speculate that the structure of the Al–Fe–Si glass is a limit of the nanostructured α -phase, with grain size as small as one unit cell, i.e. around 2 nm. This is close to the size of a fundamental structural unit – the icosahedral Mackey cluster. This structural inference has recently been strongly supported by the results of high-resolution synchrotron-based X-ray scattering and pair distribution function (PDF) analysis

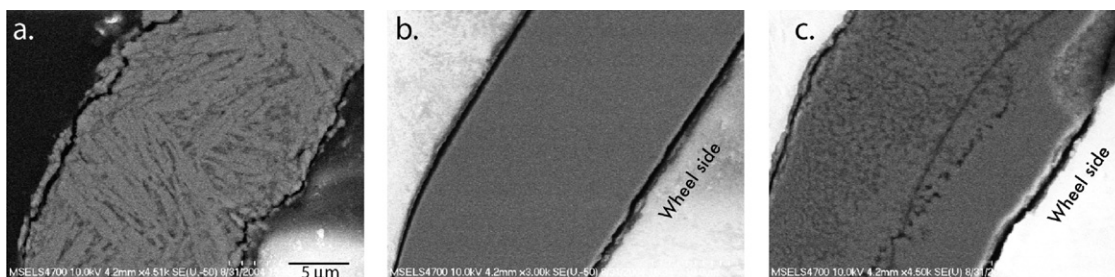


Fig. 2. Cross-sectional SEM (secondary electrons) from three different samples of the 15/20 AlFeSi alloy.

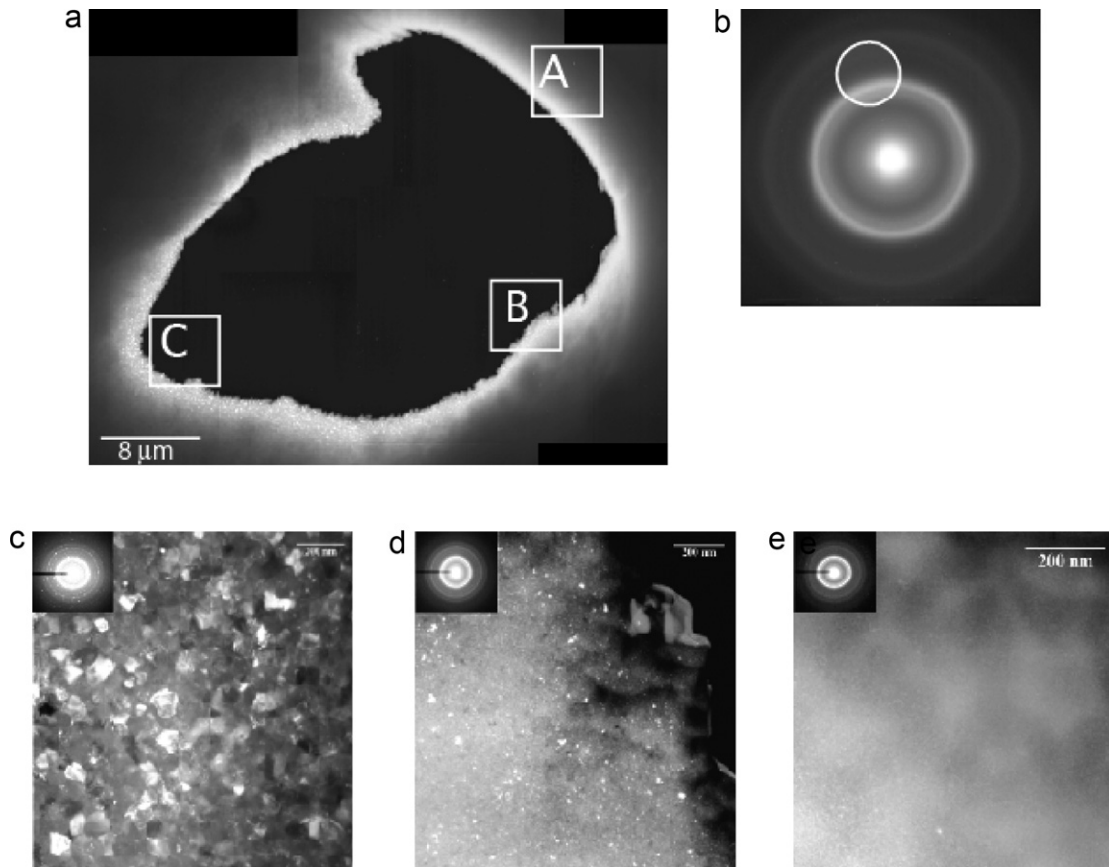


Fig. 3. (a) Low-magnification dark field TEM image showing thin area around a hole; (b) SAED pattern from (a) showing position of an aperture for dark field imaging; (c–e) dark field images of areas C, B and A, respectively.

performed on $\text{Al}_{65}\text{Fe}_{15}\text{Si}_{20}$ 100% q-glass alloys [13]; the study has shown excellent match of the experimental PDF with PDF of the nanosize α -phase. A similar conclusion has been drawn by Dubois et al. [14] in their study of amorphous $\text{Al}_{70}\text{Fe}_{13}\text{Si}_{17}$ by neutron diffraction.

Fig. 4 summarizes XRD and TEM results on the formation of microstructures in the studied Al–Fe–Si rapidly solidified alloys. There is a large compositional domain shown in Fig. 4 where QG forms with (Al) either as a secondary phase, primary or congruently. Compositions where 100% QG was found are along the boundary of the α -phase (in Fig. 1b the α phase is secondary, with primary β phase) and icosahedral phase (Fig. 1c shows nodules of icosahedral quasicrystal with Al between grains) formation. From this we conclude that QG behaves as a stoichiometric compound, with a large range of Al–Si substitution only, as shown by the dashed line in Fig. 4. Such behavior is very different from typical metallic glasses, which usually tolerate a wide range of compositions. Similar substitution of Al/Si is known for α and β Al–Fe–Si phases [15].

The selected alloys with TM=Ni, Co (atomic radius close to Fe: Ni(149 pm) < Co(152 pm) < Fe(156 pm) and compositions TM/Si = 5/8, 10/13, 13/17 and 15/20 were characterized by XRD and TEM. For both the Al–Ni–Si and Al–Co–Si systems the formation of glass was observed; however none showed the typical nodular structure of QG. At higher Al content the Al and intermetallic phases are typically formed, and at lower Al content the 100% glass structure looks like kinetically frozen liquid. The following explanations could be offered: (1) We did not succeed in reaching the exact composition-temperature window of conditions for QG formation at high Al content without interference of intermetallic phases. (2) The absence of Mackay clusters-based phases, similar to

AlFeSi α - and β -phases, in the Al–Ni–Si and Al–Co–Si systems suggests that the stability of Mackay clusters is the determining factor in the formation of QG.

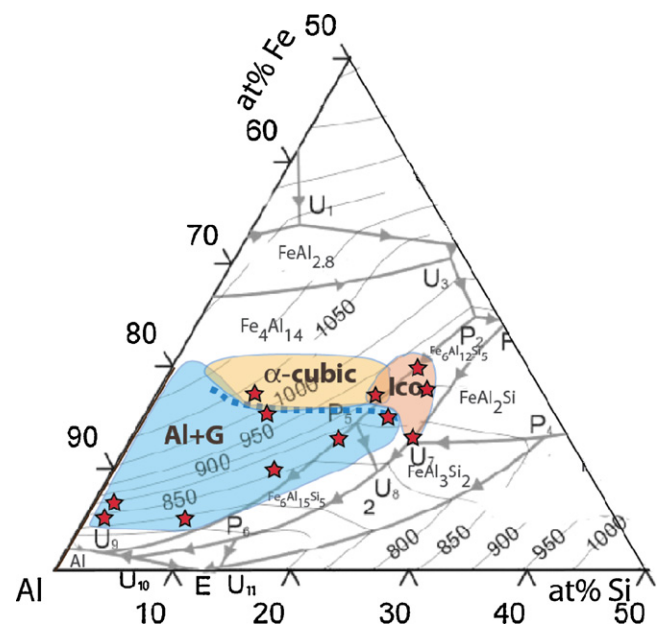


Fig. 4. Summary of XRD and TEM results showing compositional domains of formation of metastable phases in the studied Al–Fe–Si rapidly solidified alloys. Underlying diagram shows the liquidus projection where stable phases are formed [8].

4. Summary

1. The domain of Al–Fe–Si compositions where the QG forms was established. Thermodynamically the q-glass behaves as an ordinary phase and has equilibrium (metastable) with liquid and (Al). The composition of the q-glass shows substitution of Si for Al and a narrow range of Fe (15–20 at%). Its composition is close to the Al–Fe–Si β (hexagonal) and α (cubic) phase structures that are based on large icosahedral Mackay clusters.
2. XRD and TEM-based microstructural evidence, as well as the PDF from high-energy synchrotron studies, indicate that the QG structure is based on the structural motif closely related to the Mackay cluster of the AlFeSi α -phase.
3. Formation of glass in the manner similar to the QG was not observed when different transition metals substituted Fe. Substitution with Mn results in transition to a twinned α -cubic phase and then to the AlMnSi icosahedral phase [16]. As for Ni and Co, no formation of a primary glass phase was observed. Although it is possible that the required cooling conditions were not found, we speculate that the absence (stability) of the α -cubic phase for other Al–TM–Si systems is the main reason for the absence of the QG in these cases.

Acknowledgments

The authors acknowledge Frank Biancanello for alloys' preparation and Alexander Shapiro for assisting with SEM measurements.

Appendix A. Supplementary data

Supplementary data associated with this article can be found, in the online version, at [doi:10.1016/j.jallcom.2012.01.056](https://doi.org/10.1016/j.jallcom.2012.01.056).

References

- [1] L.A. Bendersky, A.J. McAlister, F.S. Biancanello, *Metall. Trans. A* 19A (1988) 2893.
- [2] L.A. Bendersky, M.J. Kaufmann, W.J. Boettinger, F.S. Biancanello, *J. Mater. Res. Sci. Eng.* 98 (1988) 213.
- [3] J.W. Cahn, L.A. Bendersky, *Mater. Res. Soc. Symp.* 806 (2004) MM2.7.1.
- [4] L.A. Bendersky, A.J. Shapiro, NIST, unpublished results, 2003.
- [5] R.O. Suzuki, Y. Komatsu, K.F. Kobayashi, P.H. Shingu, *J. Mater. Sci.* 18 (1983) 1195.
- [6] J.M. Legresy, M. Audier, J.P. Simon, P. Guyot, *Acta Metall.* 9 (1986) 1759.
- [7] M. Cooper, *Acta Crystallogr.* 23 (1967) 61106.
- [8] G. Ghosh in, G. Petzow, G. Effenberg (Eds.), *Ternary Alloys*, vol. 5, VCH Verlagsgesellschaft, 1991, pp. 394–438.
- [9] V.G. Rivlin, G.V. Raynor, *Int. Met. Rev.* 3 (1981) 133.
- [10] J. Lacaze, L. Eleno, B. Sundman, *Metall. Mater. Trans. A* 41 (9) (2010) 2208.
- [11] M. Cooper, K. Robinson, *Acta Crystallogr.* 20 (1966) 614; K. Sugiyama, N. Kaji, K. Hiraga, *Acta Crystallogr.* C54 (1998) 445.
- [12] L.A. Bendersky, F.S. Biancanello, R.J. Schaefer, *J. Mater. Res.* 2 (1987) 427.
- [13] K.W. Chapman, P. Chupas, G.G. Long, L.A. Bendersky, L.E. Levine, F. Mompiou, J.K. Stalick, J.W. Cahn, unpublished results, 2011.
- [14] J.M. Dubois, K. Dehghan, P. Chieux, M. Laridjani, *J. Non-Cryst. Solids* 93 (1987) 179.
- [15] J.E. Tibballs, R.L. Davis, B.A. Parker, *J. Mater. Sci.* 24 (1989) 2177.
- [16] L.A. Bendersky, J.W. Cahn, D. Gratias, *Philos. Mag.* B 60 (1989) 873.